 Human Molecular Genetics, 2002, Vol. 11, No. 14 **1605–1614**

Survival motor neuron (SMN) protein: role in neurite outgrowth and neuromuscular maturation during neuronal differentiation and development

Li Fan and Louise R. Simard*

Centre de Recherche, Hôpital Sainte-Justine, Montréal, Québec, Canada H3T 1C5

Received January 10, 2002; Revised and Accepted April 24, 2002

Childhood spinal muscular atrophy (SMA) is a common neuromuscular disorder caused by absent or deficient full-length survival motor neuron (SMN) protein. Clinical studies and animal models suggest that SMA is a developmental defect in neuromuscular interaction; however, the role of SMN in this process remains unclear. In the present study, we have determined the subcellular localization of SMN during retinoic-acid-induced neuronal differentiation of mouse embryonal teratocarcinoma P19 cells as well as in skeletal muscle during the critical period of neuromuscular maturation. We demonstrate, for the first time, SMN accumulation in growth-cone- and filopodia-like structures in both neuronal- and glial-like cells, identifying SMN as a new growth cone marker. Indeed, SMN was present at the leading edge of neurite outgrowths, suggesting that SMN may play a role in this process. In addition, SMN was detected as small dot-like particles within the cytoplasm of skeletal muscle during the first 2 weeks after birth, but their number peaked by P6. Intense SMN staining in neuromuscular junctions was observed throughout the entire postnatal period examined. Taken together, these results suggest that SMN may indeed fulfill neuronal- and muscle-specific functions, providing a more plausible mechanism explaining motor neuron degeneration and associated denervation atrophy of skeletal muscles in SMA. The primary SMA pathology most likely initiates in the peripheral axon – the result of deficient neurite outgrowth and/or neuromuscular maturation.

INTRODUCTION

Spinal muscular atrophy (SMA) is an autosomal recessive disorder characterized by degeneration of alpha motor neurons in the spinal cord and by muscular atrophy of the limbs and trunk. SMA is the second most common neuromuscular disease, affecting approximately 1 in 10 000 live births (1). Three clinical types are recognized based on age of onset and severity of symptoms: type I is the most severe, type II is of intermediate severity while type III is the mildest form of the disease (2,3). The causal survival motor neuron (*SMN*) gene was isolated in 1995 from a complex region of chromosome 5q13 that contains an inverted duplication of about 500 kb (4). The *SMN1* gene is telomeric of the *SMN2* gene and *SMN1* is deleted or mutated in more than 90% of all SMA patients (4,5). In addition, a number of small intragenic mutations have been documented providing conclusive evidence that *SMN1* mutations are a necessary and sufficient cause of 5q-SMA (6,7). Consistently, SMN protein is significantly reduced in fibroblast and lymphoblast cell lines from severely affected SMA patients (8,9). Although much progress has been made towards characterizing the genomic structure (4,10–12), causal mutations (5) and phenotype/genotype relationships (13), the function of SMN is not fully understood and therefore the pathogenesis of SMA remains unclear. SMN interacts or associates with several proteins, including SMN-interacting protein 1 (SIP1/Gemin2), spliceosomal U snRNP-protein, the putative helicase Gemin3, Gemin4 and many others (14–17). The large, highly stable SMN complex can be found in both cytoplasmic and nuclear compartments (9,14,17). The cytoplasmic complex plays an essential role in spliceosomal snRNP biogenesis and is required for the transport of the snRNP complex into the nucleus (17). Within the nucleus, SMN was first detected in intensely stained foci (baptized as gems for 'Gemini of coiled bodies') in close association but distinct from coiled bodies (18). Cajal (coiled) bodies (CBs) are transcription-dependent 0.5–1 μM nuclear organelles observed as tangles of coiled electron-dense threads (19), and are thought to be involved in snRNP biogenesis, transport or cycling (20). It has since been demonstrated that, for the most part, SMN co-localizes in CBs (19–22). In the nucleus, SMN is required for regenerating an active splicing complex (23,24). Consistent with the housekeeping function of SMN, it is ubiquitously expressed (8,25), and knocking out the single copy (26) mouse

*To whom correspondence should be addressed at: Centre de Recherche de l'Hôpital Sainte-Justine, 3175 Côte Sainte-Catherine, Montréal, Québec, Canada H3T 1C5. Tel: +1 514 3454931 ext 2867; Fax: +1 514 3454801; Email: simardlo@medclin.umontreal.ca

Smn gene causes developmental arrest and embryonic death (27,28). While the subcellular distribution of SMN has been extensively studied in cultured cells (8,9,22,29–31), as well as in fetal (22,25,29) and adult tissues (29,32,33), no other function, except for its housekeeping role in the splicing pathway, has yet been discovered.

If *SMN* is simply a housekeeping gene, why are neurons the main target of SMN deficiency? Do motor neurons require large amounts of SMN in excess of that required by other cell types, or does SMN fulfil a neuronal-specific function? The main feature distinguishing neurons from other cell types is that they possess dendrites and axons that convey messages from one neuron to another or target muscle cells by chemical and electrical processes. We hypothesized that SMN may have at least two functions: the first is the previously identified housekeeping function; the second may be specific to neurons. More importantly, this neuron-specific function may be related to neuronal development, because *SMN* has been shown to be developmentally regulated (34,35) and SMA may well be a developmental defect (36). To date, investigations pertaining to SMN function have been performed using cultured cell lines (8,9,22,29–31), neurons (29) or tissues (22,25,29,32,33). The cell lines employed (e.g. fibroblasts, amniocytes or HeLa cells) were not neuronal in origin and could not be induced to differentiate into neuronal cell types. Neuronal cells isolated from spinal cord are already differentiated; therefore, one cannot study SMN localization during early stages of neuronal differentiation. In studies using human, mouse or rat tissues, the resolution of detailed cell–cell interactions is limited. Consequently, we have exploited the *in situ* model of mouse embryonal teratocarcinoma P19 cells (37) to study the subcellular compartmentalization of SMN during neuronal differentiation. P19 cells can be induced to differentiate into neurons, glial cells and fibroblasts when exposed to the vitamin A analog retinoic acid (RA) in the 10^{-8}–10^{-6} M range (38,39), and RA-induced neuronal differentiation closely resembles that observed for embryonic neuroectoderm *in vivo* (40,41). To further understand the role of SMN during maturation of motor neurons and muscle, we analyzed neuromuscular junctions (NMJ) of mouse skeletal muscle isolated during the postnatal period. Our data demonstrate, for the first time, that SMN accumulates in growth-cone-like structures during neuronal differentiation, making SMN a new marker of growth cones. Furthermore, we demonstrate that in muscle, cytoplasmic SMN content peaked at postnatal day 6 just prior to the maturation of the NMJ. These observations suggest that SMN may indeed carry out a neuronal- and muscle-specific function during the maturation of neurons, muscle and NMJs.

RESULTS

Abundance of SMN-positive CBs is related to cell cycle and cell lineage

As the first step towards investigating SMN expression during early neuronal cell differentiation, we analyzed undifferentiated P19 cells for the presence of SMN protein by indirect immunofluorescence staining using a monoclonal antibody against amino acids 14–174 of human SMN. We detected diffuse SMN staining within the cytoplasm (Fig. 1A, C) as well as one to three foci of intense SMN staining on average within the nucleus (Fig. 1A, Table 1). To determine whether SMN was present in gems or CBs, double labeling of SMN and p80 coilin was undertaken, since p80 coilin is a marker of CBs. The distribution of CBs was coincident with SMN-positive nuclear foci, suggesting that both proteins co-localized within CBs (Fig. 1B, Table 1). Interestingly, 0.1–1% of cells harbored 15 or more SMN-positive CBs within the nucleus as well as intense, diffuse SMN staining in the cytoplasm (Fig. 1C, D). Because CBs associate and dissociate during the cell cycle (18,20), we first sought to determine if the presence of abundant SMN-positive CBs correlated with a specific stage of the cell cycle. To this end, P19 cells were deprived of serum for 18 hours to arrest cells in the G_0 state. Fluorescence-activated cell sorting (FACS) indicated that 44% of cells were in G_0–G_1 at this time. In general, we observed an average of 0–1 SMN/coilin foci at time 0 and an average of 1–3 SMN/coilin foci 4 and 6 hours after cells were released from serum starvation (Table 1). The rare cells containing numerous SMN-positive CBs appeared at the 6-hours time point, and DAPI staining revealed condensed chromatin suggestive of mitotic cells. As the abundance of cells with numerous SMN foci did not vary with cell state, we used GFAP and NF antibodies as markers of glial- and neuronal-like cells, respectively, to identify the specific lineage of this subpopulation of cells. After RA-induced differentiation, the numerous SMN foci were also detected in the cytoplasm (Fig. 1E), and these cells were found to be positive for GFAP (Fig. 1F, G), indicating that they were glial-like in origin. SMN foci in the cytoplasm lacked p80 coilin (data not shown).

Dynamic distribution of SMN protein during P19 neuronal differentiation

To study SMN expression during early neuronal differentiation, P19 cells were treated with RA, which triggers these cells to differentiate into several different cell types. After 10 days of treatment, neuronal- and glial-like cells appeared. SMN protein was present throughout the cytoplasm of all cells examined, and, interestingly, SMN protein accumulated in growth-cone-like structures and varicosities of neuronal-like cells during the formation of neurite processes (Fig. 2A, B). We confirmed that these cells were indeed neuronal-like in origin, since they were positive for the presence of NF-L (Fig. 2C, D). Not only were SMN and NF-L protein abundant in growth-cone-like structures, but also, in some cells, we detected a number of intensely staining SMN aggregates in the soma (Fig. 2E, F). Given the abundance of actin in neurites and growth cones, the distribution of SMN and actin was assessed by superimposing images of SMN and Texas Red-X phalloidin staining – the later binding F-actin. In contrast to the F-actin image, which shows that phalloidin staining becomes gradually faint towards to the tip of the growth-cone-like structure (Fig. 2G, H), SMN staining was more intense at the leading edge of the growth-cone-like structure (Fig. 2I, J). At day 20 post-RA treatment, neurites formed a dense network, and we no longer detected intense SMN accumulation – consistent with the loss of growth cones during neuronal maturation. Interestingly, we also detected intense SMN staining in filopodia structures of some glial-like cells (data not shown). Finally, a polyclonal antibody raised against growth-associated protein

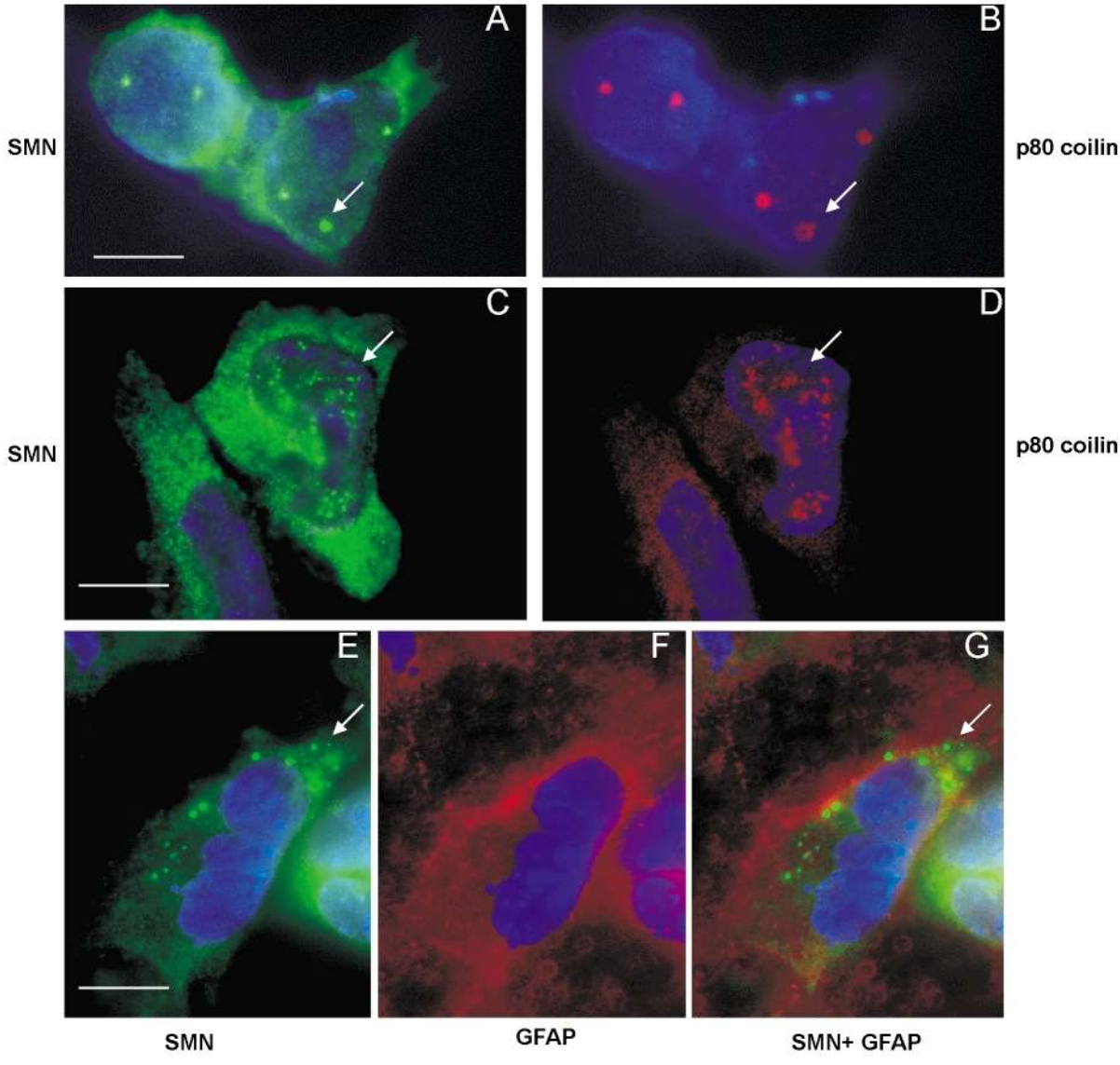

Figure 1. Indirect immunofluorescence of endogenous SMN in undifferentiated (**A**–**D**) and RA-treated (**E**–**G**) mouse P19 embryonal carcinoma (EC) cells. Cells were double-stained with a monoclonal antibody against SMN and either the rabbit polyclonal antibody R288 against p80 coilin or a polyclonal antibody against GFAP. Nuclei were stained with DAPI (blue). (A) Intense-SMN (green) staining was detected in the nucleus and diffuse SMN staining in the cytoplasm. (B) A similar number of coilin-positive CBs (red) were detected in the same cells, suggesting that SMN and p80 coilin localized in the same structure. (C) About 0.1–1% of cells harbored numerous SMN (green) foci, and (D) their distribution was coincident with CBs (red) shown in the same field. (E) After RA treatment, numerous SMN foci (green) were also detected in the cytoplasm (arrow). (F) A polyclonal antibody against GFAP (red) was used to label glial-like cells. (G) The superimposed image of a cell stained with anti-SMN (green) and anti-GFAP (red), a glial cell marker, indicated that cells with 15 or more SMN foci are glial-like in origin. Scale bars: 10 μm.

43 (GAP-43), a major component of motile growth cones (42), was employed to confirm the presence of SMN in growth-cone-like structures. A superimposed image of a differentiated P19 cell labeled with SMN (Fig. 3A) or GAP-43 (Fig. 3B) antibodies indicated that SMN and GAP-43 localized within growth cones (Fig. 3C).

Downregulation of SMN protein in muscle occurs upon maturation of the neuromuscular junction

To investigate whether SMN protein could also be involved in the maturation of the NMJ, immunofluorescence studies were carried out to detect SMN in skeletal muscle and, more specifically, NMJs during the newborn period. DAPI was used to stain nuclei, while rhodamine-conjugated α-bungarotoxin (α-BT) was used to stain NMJs (Fig. 4). Immunocytochemistry revealed intense, diffuse SMN staining and small dot-like particles throughout the cytoplasm of muscle cells and around the nuclear envelope at days 1, 3, 6 and 15 after birth. On day 1, numerous large, round nuclei were centrally located in immature muscle cells (Fig. 4A). We also observed small dot-like SMN particles against a background of diffuse SMN staining within the cytoplasm. The number of SMN particles increased by day 3 (Fig. 4B) and peaked on day 6 (Fig. 4C),

Table 1. Number of SMN and coilin foci in undifferentiated P19 cells

Hours after serum starvation period[a]	SMN foci per cell[b]	Coilin foci per cell[c]
0	0.00 ± (0,1)	0.00 ± (0,1)
4	1.00 ± (0.5,2)[d]	2.00 ± (1,2)[d]
6	1.00 ± (0,1.5)[d]	1.00 ± (0,2)[d]

[a]Undifferentiated P19 cells were deprived of serum for 18 hours to arrest cells in the G_0 state. The time indicated is that after replenishing medium with 10% FBS.
[b]SMN foci were detected by immunofluorescence staining with a monoclonal anti-SMN antibody. A total of 100 cells were scored at each time point. Data are represented as medium ± 25%, 75% distributions.
[c]CBs were detected by immunofluorescence staining with a polyclonal antibody R288 against p80 coilin. A total of 100 cells were scored at each time point. Data are represented as medium ± 25%, 75% distributions.
[d]$P < 0.0001$. Significance, compared with 0 hour, was determined by a Mann–Whitney Rank Sum test. *P*-values less then 0.05 are considered to be statistically significant.

and, by day 15, we observed a dramatic decrease in the intensity of the diffuse cytoplasmic staining as well as in the number SMN particles in mature muscle cells, which contained flattened, peripherally located nuclei (Fig. 4D). Double labeling with SMN antibody and α-BT indicated that SMN was always highly expressed at the NMJ throughout the stages tested (Fig. 4).

DISCUSSION

Clinical studies (reviewed in 36), coupled with data from recently developed animal models (43–45), point towards the possibility that SMA is a developmental defect in neuromuscular interaction (46). However, evidence implicating SMN in this process has been hampered by the fact that the majority of studies to date have employed non-neuronal cell lines (14,15,17) or by the limited ability to resolve cell–cell interactions from tissue sections (22,25,29,31,32,47–50). Consequently, we have investigated the subcellular localization of SMN during neuronal differentiation and neuromuscular maturation to determine if SMN possesses a neuronal- and/or muscle-specific function. To achieve this goal, we have analyzed undifferentiated and RA-induced P19 cells as well as skeletal muscle tissue sections during the critical period of NMJ maturation. As in other cell types, SMN was scattered throughout the cytoplasm, and, in the nucleus, SMN was found to be coincident with CBs in P19 cells. The number of CBs per cell was not static, but varied throughout the cell cycle. In undifferentiated P19 cells, we detected an average of 0–1 SMN/coilin foci immediately after 18 hours of serum starvation compared with 2–3 SMN/coilin foci detected 4 and 6 hours after cells were released into fully supplemented media. This is in agreement with the observed cell-cycle-dependent variation in the distribution of p80 coilin, a marker of CBs, in mouse 3T3 fibroblasts and HeLa S3 cells – the number of CBs being most abundant in late G_1 (51). Our data are consistent with previous studies indicating that SMN is generally found in CBs (19–22), and this subcellular localization is most likely related to the housekeeping function of SMN in snRNP biogenesis and regeneration of the splicing complex (17,23). Given that glial cells represent at least 50% of the total cell population, one unexpected observation was the presence of more than 15 SMN/coilin foci in the cytoplasm and/or nucleus in only 0.1–1% of glial-like cells. Further studies are required to determine whether these cells are simply a cell culture artifact or whether they represent a distinct subpopulation of glial cells expressing abundant amounts of SMN.

Our most striking finding was the redistribution and accumulation of cytoplasmic SMN at the periphery of the cell body and in growth-cone- and filopodia-like structures in both neuronal- and glial-like cells. Subcellular localization in growth cones was confirmed by demonstrating the presence of GAP-43, a protein involved in neurite outgrowth (42), along neurite processes and localization of both SMN and GAP-43 within growth cones. Because immunoelectron microscopy suggests that SMN particles may be associated with microtubules in dendrites (48), we speculate that SMN may be transported along microtubules, relocalizing it within growth cones. Growth cones are dynamic structures that respond to intra- and extracellular cues to guide neurites towards an appropriate target during neuronal development (52). Growth cones with the simplest morphology are those whose neurites are extending rapidly (53) and are most similar to the simple shapes that we observed in our RA-treated P19 cells. Superimposed images of F-actin and SMN staining showed SMN at the leading edge of neurite outgrowths, suggesting that SMN may play a role in this process. It is well established that SMN interacts with a number of proteins, many of which have not yet been identified (17). Interestingly, profilin II, a motoneuron-specific microfilament-associated, actin-binding protein involved in actin polymerization (54,55), has been shown to interact directly with SMN via the evolutionarily conserved Pro_5-X_{17}-Pro_{10}-X_{17}-Pro_5 motif (56) encoded by exons 4, 5 and 6 of the *SMN* gene (4,26). This interaction may mediate actin and SMN transport in neurite outgrowths. These data suggest that SMN deficiency could result in a defect in maturation of motor neurons, which in turn would impact on muscle maturation. Consistently, it has been established that muscle atrophy precedes loss of motor neurons using two distinct SMA animal models (43,44). In the first model, $SMN^{F7/\Delta7}$, Cre^{+} mice homozygous for deletions of *SMN* exon 7 in neurons only, indicated that NMJs were morphologically abnormal by 2 weeks of age, but that the number of spinal cord motor neurons was normal – indicating that the observed muscle phenotype was neurogenic in origin (43). By 4 weeks of age, motor neurons were markedly deformed. In the second model, the human *SMN2* gene was introduced into the $Smn^{-/-}$ background ($Smn^{-/-}$,*SMN2*), thereby producing mice with a genotype that most closely resembled that of type I SMA patients (44). Similarly, the number of motor neurons was initially normal, and motor neuron loss began after P3 in low-copy $Smn^{-/-}$, *SMN2* mice; however, muscle weakness was evident at birth. Based on these results, we speculate that SMA pathology starts within distal processes, progresses towards the soma of developing neurons, and motor neuron cell death most likely results from the lack of SMN in growth cones and improper maturation of the NMJ. Consistent with the ability of SMN to bind both proteins (17) and RNA (57,58), we also speculate that SMN may be involved in the transport of these molecules to the periphery of neurites, thereby ensuring an

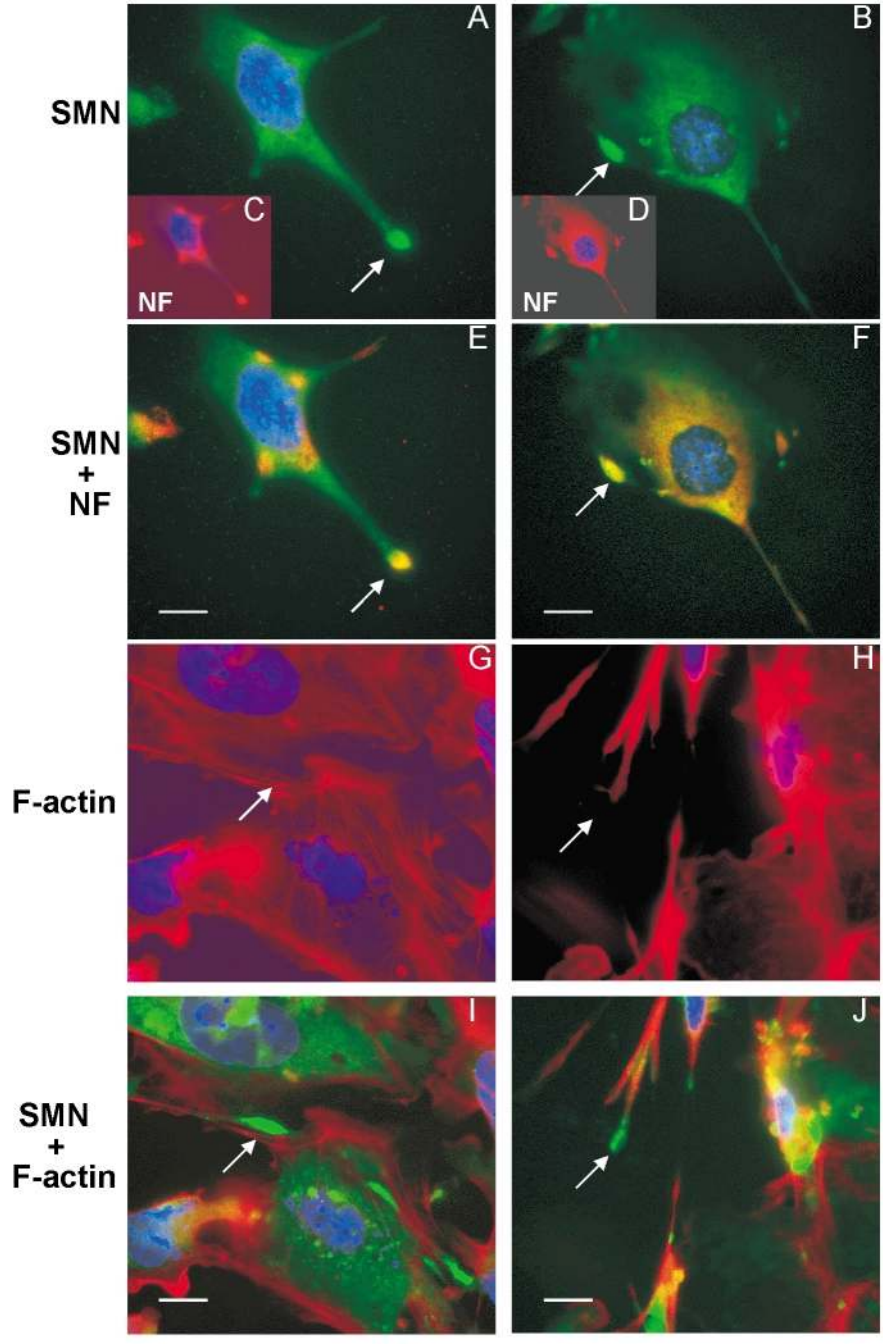

Figure 2. SMN in differentiating neuronal-like P19 cells aggregates in growth-cone-like structures. Cells were immunostained with a monoclonal antibody against SMN and either a rabbit polyclonal antibody against neurofilament 68 kDa (NF-L) or an F-actin marker, Texas Red-X phaloidin. Nuclei were counterstained with DAPI (blue). (**A**, **B**) SMN (green) accumulates in growth-cone-like structures (arrow) and at the periphery of the soma. (**C**, **D**) Diffuse NF-L (red) staining was observed throughout the cytoplasm, the labeling being more intense at the periphery of the soma as well as the tips of neurite processes. (**E**, **F**) Superimposed images of double-labeled cells with anti-SMN and NF-L, demonstrating that SMN aggregated in the soma and growth-cone-like structures and that these cells are rich in NF-L (yellow). (**G**, **H**) Abundant F-actin was detected except at the tip of growth-cone-like structures (arrow). (**I**, **J**) Superimposed images showing SMN (green) and F-actin (red) in the cell body and growth-cone-like structure (arrow), where co-localization of SMN and F-actin appears in yellow. Scale bars: 10 μm.

adequate pool of proteins in high demand during growth-cone formation and early neuronal development. There is mounting evidence indicating that mRNA targeting to synapses and local protein synthesis is involved in neuronal polarity, synaptic plasticity and possibly long-term memory (59–62). This hypothesis is consistent with the recent identification of two additional SMN partners (63,64), namely the RNA-binding proteins hnRNP-R and hnRNP-Q, coupled with the demonstra-

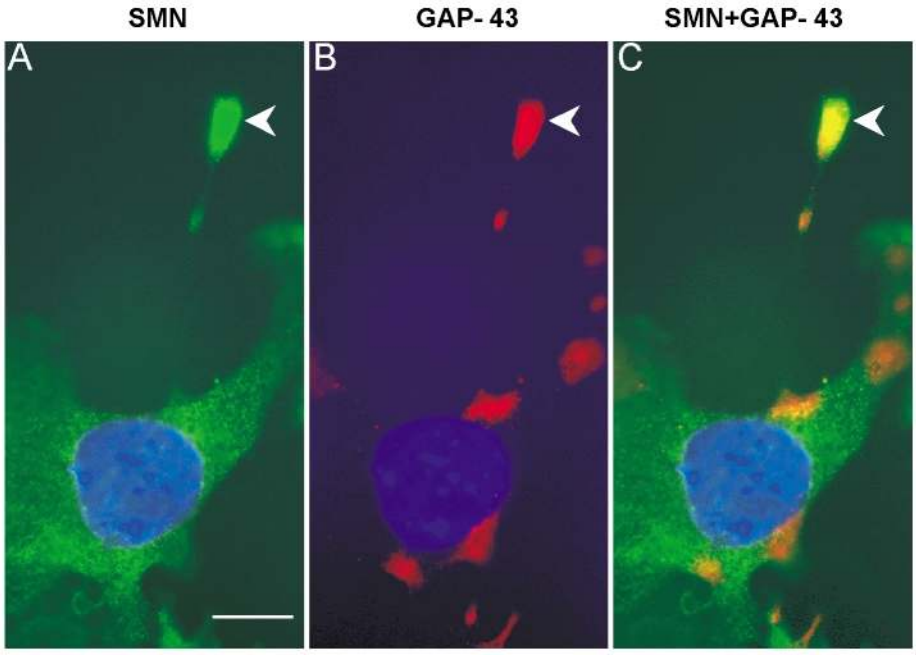

Figure 3. Distribution of SMN and GAP-43 in RA-treated P19 cells. (**A**) Diffuse SMN (green) staining was detected throughout the cytoplasm, and accumulated in growth-cone-like structures. (**B**) GAP-43 (red) aggregated at the periphery of the soma and along neurite processes. As expected, labeling was most intense within the growth cone. (**C**) Superimposed image indicating coincident staining (yellow) of SMN and GAP-43, with intense labeling of the growth cone. Arrowheads point to growth-cone-like structures. Scale bar: 10 μm.

tion that SMN and hnRNP-R co-localize in distal axons of embryonic motor neurons (64).

The amount and subcellular localization of SMN varied during early mouse skeletal muscle development, which is consistent with previous reports indicating downregulation of SMN expression during myogenesis *in vitro* (25) and in comparisons of fetal and adult skeletal muscle (32). We detected diffuse staining and numerous small dot-like SMN particles in skeletal muscle cytoplasm, as well as intense SMN staining in NMJs during the first 2-weeks of postnatal life; however, once matured, the intensity of cytoplasmic staining and number of dot-like SMN particles decreased drastically while SMN remained concentrated in the NMJ. These results suggest that the presence of SMN in muscle may also be important during this critical period. In rodents, the complex process interconnecting motor neurons and skeletal muscle requires 2–3 weeks and initiates around embryonic day 13, as motor axons enter developing muscle masses, and terminates around P14, when the mature muscle fiber is innervated by a single motor axon (65–67). Blocking this process causes retraction of the axon and leads to motor neuron cell death (46). Consequently, functional interaction between the motor neuron and its target muscle is critical in determining whether a given motor neuron will mature sufficiently to contribute to the CNS. This, and our data localizing SMN in growth-cone-like structures during neuronal cell differentiation, suggest that SMN may play a role during NMJ maturation. This hypothesis is supported by previous demonstrations of a sharp decrease in spinal cord and muscle SMN in rodents during the first 2 weeks of life (50,68) and further supported by SMA animal models indicating that muscle atrophy precedes motor neuron loss (43,44), the presence of muscle atrophy in mice lacking SMN specifically in muscle (45) and the more severe phenotype in the low-copy $SMN^{-/-}$, *SMN2* mice deficient for SMN in both neurons and muscle (28,44).

In summary, our present study provides strong evidence for the accumulation of SMN in growth cones and NMJs during neuronal differentiation and neuromuscular maturation, suggesting that cytoplasmic SMN may indeed possess a neuronal- and muscle-specific function. Because RA-induced P19 cells mimic normal neuronal cell differentiation (40,41), we believe that these results accurately reflect the relocalization of SMN during this process, and this premise is further supported by the predominance of SMN in the cytoplasm of motor neurons (25,32,47), the presence of SMN in axons and dendrites (29,31,50,64), as well as independent localization of SMN in the NMJ (49). This function is associated with full-length SMN, given the mouse origin of P19 cells. The existence of a neuronal- and muscle-specific role for SMN provides a more plausible mechanism explaining motor neuron degeneration and associated denervation atrophy of skeletal muscles in SMA. Indeed, disease severity may reflect the state of muscle maturation and extent of motor neuron death during development, as previously proposed (69). In conclusion, SMN deficiencies in neurons, glial cells and muscle may each contribute to the pathogenesis of SMA, and future studies should focus on the cytoplasmic function of SMN in these cell lineages if we are to make further progress in our understanding of SMA etiology.

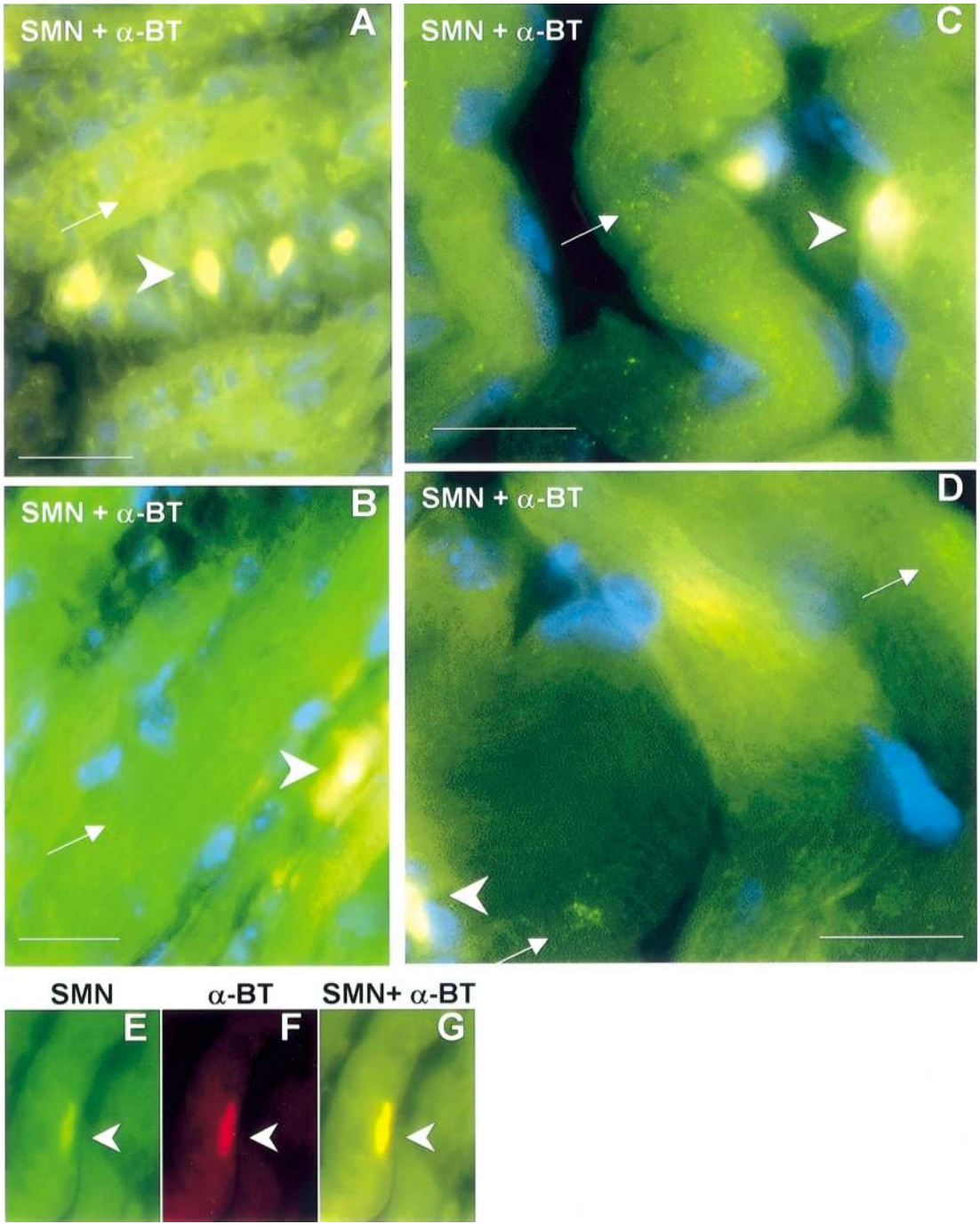

Figure 4. Double immunofluorescence labeling of SMN in postnatal day 1 (**A**), 3 (**B**), 6 (**C**) and 15 (**D**) muscle. SMN was revealed with a monoclonal anti-SMN antibody (green), while NMJs were labeled with α-bungarotoxin (α-BT: red). SMN aggregated into numerous bright dot-like particles (arrows) in the cytoplasm of muscle cells. Note that peak expression occurred at day 6 (C). (**E**) A day-3 muscle showing diffuse cytoplasmic labeling in addition to intense accumulation of SMN (green) at the NMJ. (**F**) The same muscle cell stained with α-BT (red) to label the NMJ. (**G**) A superimposed image of the same muscle cell, showing that SMN and α-BT are coincident (yellow). Nuclei were stained with DAPI (blue). Arrowheads mark the sites of NMJs, and the yellow color indicated that SMN accumulates in these structures. Scale bars: 10 μm.

MATERIALS AND METHODS

Synchronization of P19 cells

Mouse P19 embryonal carcinoma cells (ATCC CRL-1825) were maintained in α-minimum essential medium (α-MEM) supplemented with 10% (v/v) fetal bovine serum (FBS) at 37°C in a 5% CO_2 incubator. Synchronization of P19 cells was carried out by serum deprivation. Cells were grown to 50% confluency and placed in α-MEM containing 0.5% FBS, and after 18 h starvation, the serum-deficient medium was replaced by α-MEM containing 10% FBS. Cells were fixed every hour

for more than 10 h after replenishing cells with 10% FBS. 100 cells were examined per time point to determine the proportion of mitotic cells in the total cell population as well as the number of SMN foci and CBs per cell. Mitosis was monitored by 4′,6-diamidino-2-phenylindole dihydrochloride (DAPI; Sigma-Aldrich Co., Ontario) staining. SMN foci and CBs were revealed by double immunofluorescence labeling using a monoclonal antibody against SMN (BD PharMingen, Ontario) and the rabbit polyclonal antibody R288 against p80 coilin (a gift from Dr Edward K. L. Chan; see 51). The state of cells at the end of the serum starvation period as well as 4 and 6 h after replenishing cells with 10% FBS was established by passing 3.6×10^6 cells in Krishan solution through a FACS.

Differentiation of P19 cells

Differentiation of P19 cells with retinoic acid was based on the method previously described (70). Briefly, P19 cells (5×10^5 per petri dish) were induced to differentiate by the addition of 2 μM all-*trans*-retinoic acid (RA; Sigma-Aldrich Co., Ontario). Cells were aggregated in bacterial petri dishes and, after 48 h incubation, aggregates were dispersed with 0.125% (w/v) trypsin and 1 mM EDTA before replating on bacterial petri dishes containing α-MEM with fresh RA for a further 24 h. Small cell aggregates (50 cells or so) were picked using sterile pipette tips, seeded on poly-L-lysine-coated microscope coverslips in α-MEM with 10% FBS and grown for 3 days. Cells were then treated with 13 μg/ml of 5-fluoro-2′-deoxyuridine and 33 μg/ml uridine to suppress overgrowth of glia- and fibroblast-like cells and after 48 h returned to glutamine-free α-MEM containing 10% FBS. Medium was changed every 3–4 days, and cells were harvested on days 5, 10 and 20 after RA treatment. For undifferentiated controls, untreated P19 cells were seeded on poly-L-lysine-coated microscope cover slips and cultured for 24 h prior to immunocytochemical analysis.

Indirect immunofluorescence of P19 cells

P19 cells were rinsed twice with phosphate-buffered saline (PBS, pH 7.2) and fixed for 10 min at room temperature using freshly prepared, ice-cold 4% (w/v) paraformaldehyde in PBS, followed by three 2 min washes in PBS. Non-specific binding sites were blocked by incubation with 3% (v/v) normal goat serum for 1 h at room temperature. Samples were then incubated overnight at 4°C with primary antibodies, followed by four 5 min washes in PBS. The primary antibodies used in these studies were a monoclonal antibody against human SMN (generated against a polypeptide corresponding to amino acids 14–174 of SMN) and rabbit polyclonal antibodies against p80 coilin (R288), 68 kDa neurofilament (NF-L; Chemicon International, Inc., CA), glial fibrillary acidic protein (GFAP; DAKO, CA) and growth associated protein 43 (GAP-43; Chemicon International, Inc., CA). Secondary antibodies were applied for 2 h at room temperature individually for single-labeling experiments or as a mixture for double-labeling experiments, followed by four 5 min washes in PBS. Secondary antibodies included goat anti-mouse IgG (H + L) coupled to Cy2 as well as goat anti-rabbit IgG (H + L) coupled to Cy3 (Jackson ImmunoResearch Laboratories, PA). To label F-actin, cells were incubated for 1 h with Texas Red-X phalloidin (Molecular Probes, OR), together with secondary antibody at room temperature. The primary and secondary antibodies, as well as the F-actin marker, were diluted in PBS in the presence of 3% (w/v) bovine serum albumin (BSA). Cell nuclei were counterstained with 50 nM DAPI in PBS for 5 min, followed by four 5 min washes in PBS. Controls were performed by using normal rabbit serum or by omitting the first antibody. Finally, samples were mounted with a glycerol solution (1/9 dilution in PBS) and examined by fluorescence microscopy (Nikon ECLIPSE E600, Japan) using Zeiss software (AxioVision 2.05, Carl Zeiss GmbH, Germany). Excitation wavelengths were set at 540–580 nm for Cy3, 460–500 nm for Cy2 and 330–380 nm for DAPI staining. No extra modifications were made on any of the fluorescent images; however, images were superimposed using Zeiss software in the case of double-labeling experiments.

Indirect Immunofluorescence of muscle

Postnatal mice (days 1, 3, 6 and 15) were killed by cervical dislocation. Rectus femoris and gastrocnemius muscles were dissected from the hind leg. Striated muscle was rinsed several times in PBS before overnight fixation with 4% (w/v) paraformaldhyde. Fixed samples were rinsed in PBS and dehydrated by 5 min incubations through a series of 70%, 80%, 90%, 95%, and 100% ethanol and absolute toluene, followed by embedding in paraplast (Sigma-Aldrich Co., Ontario). Samples were sectioned at 6 μm; paraplast was removed by immersing slides for 15 min in toluene and sections were rehydrated in decreasing serial concentrations of ethanol. Samples were then incubated with 1% SDS in Tris-buffered saline for 5 min, and double labeling of the NMJ was done by incubation with the primary anti-SMN antibody followed by treatment with 0.5 μg/ml tetramethylrhodamine-conjugated α-bungarotoxin (Molecular Probes) and the secondary goat anti-mouse IgG (H + L) coupled to Cy2. The excitation wavelength for tetramethylrhodamine was 540–580 nm. Nuclei were counterstained with DAPI.

ACKNOWLEDGEMENTS

We are grateful to Drs E.M. Tan and E.K. Chan for providing the polyclonal antibody against p80 coilin. We thank C. Rochette for technical assistance, Dr A. Pshezhetsky for advice on computational microscopy, Marie Blagdon for FACS analysis, and Drs P. Wilce, B. Key and M. Emond for helpful discussion. This work was supported by grants from Families of SMA and the Canadian Institutes of Health Research. L.R.S. is a Fonds de la Recherche en Santé du Quebec Scholar.

REFERENCES

1. Pearn, J. (1978) Incidence, prevalence and gene frequency studies of chronic childhood spinal muscular atrophy. *J. Med Genet.*, **15**, 409–413.
2. Munsat, T.L. and Davies, K.E. (1992) Meeting report: International SMA Consortium Meeting. *Neuromusc. Disord.*, **2**, 423–428.
3. Dubowitz, V. (1995) Diagnosis and classification of the neuromuscular disorders. In Dubowitz, V. (ed.), *Muscle Disorders In Childhood*. W.B. Saunders, Philadelphia, pp. 2–3.
4. Lefebvre, S., Bürglen, L., Reboullet, S., Clermont, O., Burlet, P., Viollet, L., Benichou, B., Cruaud, C., Millasseau, P., Zeviani, M. *et al.* (1995)

Identification and characterization of a spinal muscular atrophy-determining gene. *Cell*, **80**, 55–165.
5. Wirth, B. (2000) An update of the mutation spectrum of the survival motor neuron gene (SMN1) in autosomal recessive spinal muscular atrophy (SMA). *Hum. Mutat.*, **15**, 228–237.
6. Bussaglia, E., Clermont, O., Tizzano, E., Lefebvre, S., Bürglen, L., Cruaud, C., Urtizberea, J.A., Colomer, J., Munnich, A., Baiget, M. and Melki, J. (1995) A frame-shift deletion in the survival motor neuron gene in Spanish spinal muscular atrophy patients. *Nat. Genet.*, **1**, 335–337.
7. Rochette, C.F., Surh, L.C., Ray, P.N., McAndrew, P.E., Prior, T.W., Burghes, A.H., Vanasse, M. and Simard, L.R. (1997) Molecular diagnosis of non-deletion SMA patients using quantitative PCR of SMN exon 7. *Neurogenetics*, **1**, 141–147.
8. Covert, D.D., Le, T.T., McAndrew, P.E., Strasswimmer, J., Crawford, T.O., Mendell, J.R., Coulson, S.E., Androphy, E.J., Prior, T.W. and Burghes, A.H.M. (1997) The survival motor neuron protein in spinal muscular atrophy. *Hum. Mol. Genet.*, **6**, 1205–1214.
9. Lefebvre, S., Burlet, P., Liu, Q., Bertrandy, S., Clermont, O., Munnich, A., Dreyfuss, G. and Melki,, J. (1997) Correlation between severity and SMN protein level in spinal muscular atrophy. *Nat. Genet.*, **16**, 265–269.
10. Chen, Q., Baird, S.D., Mahadevan, M., Besner-Johnston, A., Farahani, R., Xuan, J., Kang, X., Lefebvre, C., Ikeda, J.E., Korneluk, R.G. and MacKenzie, A.E. (1998) Sequence of a 131-kb region of 5q13.1 containing the spinal muscular atrophy candidate genes SMN and NAIP. *Genomics,* **48**, 121–127.
11. Monani, U.R., Lorson, C.L., Parsons, D.W., Prior, T.W., Androphy, E.J., Burghes, A.H. and McPherson, J.D. (1999) A single nucleotide difference that alters splicing patterns distinguishes the SMA gene SMN1 from the copy gene SMN2. *Hum. Mol. Genet.*, **8**, 1177–1183.
12. Rochette, C.F., Gilbert, N. and Simard, L.R. (2001) SMN gene duplication and the emergence of the SMN2 gene occurred in distinct hominids: SMN2 is unique to *Homo sapiens*. *Hum. Genet.*, **108**, 255–266.
13. Simard, L.R., Rochette, C., Semionov, A., Morgan, K. and Vanasse, M. (1997) SMN(T) and NAIP mutations in Canadian families with spinal muscular atrophy (SMA): genotype/phenotype correlations with disease severity. *Am. J. Med. Genet.*, **72**, 51–58.
14. Liu, Q., Fischer, U., Wang, F. and Dreyfuss, G. (1997) The spinal muscular atrophy disease gene product, SMN, and its associated protein SIP1 are in a complex with spliceosomal snRNP proteins. *Cell*, **90**, 1013–1021.
15. Charroux, B., Pellizzoni, L., Perkinson, R.A., Shevehenko, A., Mann, M. and Dreyfuss, G. (1999) Gemin3: A novel DEAD box protein that interacts with SMN, the spinal muscular atrophy gene product, and is a component of gems. *J. Cell. Biol.*, **147**, 1181–1194.
16. Charroux, B., Pellizzoni, L., Perkinson, R.A., Yong, J., Shevchenko, A., Mann, M. and Dreyfuss, G. (2000) Gemin4. A novel component of the SMN complex that is found in both gems and nucleoli. *J. Cell. Biol.*, **148**, 1177–1186.
17. Meister, G., Buhler, D., Laggerbauer, B., Zobawa, M., Lottspeich, F. and Fischer, U. (2000) Characterization of a nuclear 20S complex containing the survival of motor neurons (SMN) protein and a specific subset of spliceosomal Sm proteins. *Hum. Mol. Genet.*, **9**, 1977–1986.
18. Liu, Q. and Dreyfuss, G. (1996) A novel nuclear structure containing the survival of motor neurons protein. *EMBO J.*, **15**, 3555–3565.
19. Pena, E., Berciano, M.T., Fernandez, R., Ojeda, J.L. and Lafarga, M. (2001) Neuronal body size correlates with the number of nucleoli and Cajal bodies, and with the organization of the splicing machinery in rat trigeminal ganglion neurons. *J. Comp. Neurol.*, **430**, 250–263.
20. Carvalho, T., Almeida, F., Calapez, A., Lafarga, M., Berciano, M.T. and Carmo-Fonseca, M. (1999) The spinal muscular atrophy disease gene product, SMN: a link between snRNP biogenesis and the Cajal (coiled) body. *J. Cell. Biol.*, **147**, 715–728.
21. Matera, A.G. and Frey, M.R. (1998) Coiled bodies and gems: Janus or Gemini? *Am. J. Hum. Genet.*, **63**, 317–321.
22. Young, P.J, Le, T.T., Thi Man, N., Burghes, A.H. and Morris, G.E. (2000) The relationship between SMN, the spinal muscular atrophy protein, and nuclear coiled bodies in differentiated tissues and cultured cells. *Exp. Cell. Res.*, **256**, 365–374.
23. Pellizzoni, L., Kataoka, N., Charroux, B. and Dreyfuss, G. (1998) A novel function for SMN, the spinal muscular atrophy disease gene product, in pre-mRNA splicing. *Cell*, **95**, 615–624.
24. Fischer, U., Liu, Q. and Dreyfuss, G. (1997) The SMN–SIP1 complex has an essential role in spliceosomal snRNP biogenesis. *Cell*, **90**, 1023–1029.
25. Burlet, P., Huber, C., Bertrandy, S., Ludosky, M.A., Zwaenepoel, I., Clermont, O., Roume, J., Delezoide, A.L., Cartaud, J., Munnich, A. and Lefebvre, S. (1998) The distribution of SMN protein complex in human fetal tissues and its alteration in spinal muscular atrophy. *Hum. Mol. Genet.*, **7**, 1927–1933.
26. DiDonato, C.J., Chen, X.N., Noya, D., Korenberg, J.R., Nadeau, J.H. and Simard, L.R. (1997) Cloning, characterization, and copy number of the murine survival motor neuron gene: homolog of the spinal muscular atrophy-determining gene. *Genome Res.*, **7**, 339–352.
27. Schrank, B., Götz, R, Gunnersen, J.M., Ure, J.M., Toyka, K.V., Smith, A.G. and Sendtner, M. (1997) Inactivation of the survival motor neuron gene, a candidate gene for human spinal muscular atrophy, leads to massive cell death in early mouse embryos. *Proc. Natl Acad. Sci. USA*, **94**, 9920–9925.
28. Hsieh-Li, H.M., Chang, J.G., Jong, Y.J., Wu, M.H., Wang, N.M., Tsai, C.H. and Li, H. (2000) A mouse model for spinal muscular atrophy. *Nat. Genet.*, **24**, 66–70.
29. Francis, J.W., Sandrock, A.W., Bhide, P.G., Vonsattel, J.P. and Brown R.H. Jr, (1998) Heterogeneity of subcellular localization and electrophoretic mobility of survival motor neuron (SMN) protein in mammalian neural cells and tissues. *Proc. Natl Acad. Sci. USA*, **95**, 6492–6497.
30. Patrizi, A.L., Tiziano, F., Zappata, S., Donati, M.A., Neri, G. and Brahe, C. (1999) SMN protein analysis in fibroblast, amniocyte and CVS cultures from spinal muscular atrophy patients and its relevance for diagnosis. *Eur. J. Hum. Genet.*, **7**, 301–309.
31. La Bella, V., Kallenbach., S. and Pettmann, B. (2000) Expression and subcellular localization of two isoforms of the survival motor neuron protein in different cell types. *J. Neurosci. Res.*, **62**, 346–356.
32. Williams, B.Y., Vinnakota, S., Sawyer, C.A., Waldrep, J.C., Hamilton, S.L. and Sarkar, H.K. (1999) Differential subcellular localization of the survival motor neuron protein in spinal cord and skeletal muscle. *Biochem. Biophys. Res. Commun.*, **254**, 10–14.
33. Young, P.J., Le, T.T., Dunckley, M., Nguyen, T.M., Burghes, A.H. and Morris, G.E. (2001) Nuclear gems and Cajal (coiled) bodies in fetal tissues: nucleolar distribution of the spinal muscular atrophy protein, SMN. *Exp. Cell. Res.*, **265**, 252–261.
34. La Bella, V., Cisterni, C., Salaün, D. and Pettmann, B. (1998) Survival motor neuron (SMN) protein in rat is expressed as different molecular forms and is developmentally regulated. *Eur. J. Neurosci.*, **10**, 2913–2923.
35. Germain-Desprez, D., Brun, T., Rochette, C., Semionov, A., Rouget, R and Simard, L.R. (2001) The SMN genes are subject to transcriptional regulation during cellular differentiation. *Gene*, **279**, 109–117.
36. Crawford, T.O. and Pardo, C.A. (1996) The neurobiology of childhood spinal muscular atrophy. *Neurobiol. Dis.*, **3**, 97–110.
37. McBurney, M.W. and Rogers, B.J. (1982) Isolation of male embryonal carcinoma cells and their chromosome replication patterns. *Dev. Biol.*, **89**, 503–508.
38. McBurney, M.W., Reuhl, K.R., Ally, A.I., Nasipuri, S., Bell, J.C. and Craig, J. (1988) Differentiation and maturation of embryonal carcinoma-derived neurons in cell culture. *J. Neurosci.*, **8**, 1063–1073.
39. Staines, W.A., Morassutti, D.J., Reuhi, K.R., Ally, A.I. and McBurney, M.W. (1994) Neurons derived from P19 embryonal carcinoma cells have varied morphologies and neurotransmitters. *Neuroscience*, **58**, 735–751.
40. Staines, W.A., Craig, J., Reuhi, K. and McBurney, M.W. (1996) Retinoic acid treated P19 embryonal carcinoma cells differentiate into oligodendrocytes capable of myelination. *Neuroscience*, **71**, 845–853.
41. Bain, G., Ray, W.J., Yao, M. and Gottlieb, D.I. (1994) From embryonal carcinoma cells to neurons: the P19 pathway. *Bioessays*, **16**, 343–348.
42. Aigner, L. and Caroni, P. (1995) Absence of persistent spreading, branching, and adhesion in GAP-43 depleted growth cones. *J. Cell. Biol.*, **128**, 647–660.
43. Frugier, T., Tiziano, F.D., Cifuentes-Diaz, C., Miniou, P., Roblot, N., Dierich, A., Le Meur, M. and Melki, J. (2000) Nuclear targeting defect of SMN lacking the C-terminus in a mouse model of spinal muscular atrophy. *Hum. Mol. Genet.*, **9**, 849–858.
44. Monani, U.R., Sendtner, M., Coovert, D.D., Parsons, D.W., Andreassi, C., Le, T.T., Jablonka, S., Schrank, B., Rossol, W., Prior, T.W. *et al.* (2000) The human centromeric survival motor neuron gene (SMN2) rescues embryonic lethality in $Smn^{-/-}$ mice and results in a mouse with spinal muscular atrophy. *Hum. Mol. Genet.*, **9**, 333–339.
45. Cifuentes-Diaz, C., Frugier, T., Tiziano, F.D., Lacene, E., Roblot, N., Joshi, V., Moreau, M.H. and Melki, J. (2001) Deletion of murine SMN exon 7 directed to skeletal muscle leads to severe muscular dystrophy. *J. Cell. Biol.*, **152**, 1107–1114.

46. Greensmith, L. and Vrbova, G. (1997) Disturbances of neuromuscular interaction may contribute to muscle weakness in spinal muscular atrophy. *Neuromuscul. Disord.*, **7**, 369–372.
47. Battaglia, G., Princivalle, A., Forti, F., Lizier, C. and Zeviani, M. (1997) Expression of the SMN gene, the spinal muscular atrophy determining gene, in the mammalian central nervous system. *Hum. Mol. Genet.*, **6**, 1961–1971.
48. Bechade, C., Rostaing, P., Cisterni, C., Kalisch, R., La Bella, V., Pettmann, B. and Triller, A. (1999) Subcellular distribution of survival motor neuron (SMN) protein: possible involvement in nucleocytoplasmic and dendritic transport. *Eur. I Neurosci.*, **11**, 293–304.
49. Broccolini, A., Engel, W.K. and Askanas, V. (1999) Localization of survival motor neuron protein in human apoptotic-like and regenerating muscle fibers, and neuromuscular junctions. *Neuroreport*, **10**, 1637–1641.
50. Pagliardini, S., Giavazzi, A., Setola, V., Lizier, C., Di Luca, M., DeBiasi, S. and Battaglia, G. (2000) Subcellular localization and axonal transport of the survival motor neuron (SMN) protein in the developing rat spinal cord. *Hum. Mol. Genet.*, **9**, 47–56.
51. Andrade, L.E., Tan, E.M. and Chan, E.K. (1993) Immunocytochemical analysis of the coiled body in the cell cycle and during cell proliferation. *Proc. Natl Acad. Sci. USA*, **90**, 1947–1951.
52. Berman, S.A., Moss, D. and Bursztajn, S. (1993) Axonal branching and growth cone structure depend on target cells. *Dev. Biol.*, **159**, 153–162.
53. Raper, J.A. and Tessier-Lavigne, M. (1999) Growth cones and axon pathfinding. In Zigmond, M.J., Bloom, F.E., Landis, S.C., Roberts, J.L. and Squire, L.R. (eds). *Fundamental Neuroscience.* Academic Press, New York, pp. 520–521.
54. Lambrechts, A., Verschelde, J.-L., Jonckheere, V., Goethals, M., Vandekerckhove, J. and Ampe, C. (1997) The mammalian profilin isoforms display complementary affinities for PIP_2 and proline-rich sequences. *EMBO J.*, **16**, 484–494.
55. Lambrechts, A., Braun, A., Jonckheere, V., Aszodi, A., Lanier, L.M., Robbens, J., van Colen, I., Vandekerckhove, J., Fässler, R. and Ampe, C. (2000) Prolifin II is alternatively spliced, resulting in prolifin isoforms that are differentially expressed and have distinct biochemical properties. *Mol. Cell. Biol.*, **20**, 8209–8219.
56. Giesemann, T., Rathke-Hartlieb, S., Rothkegel, M., Bartsch, J.W., Buchmeier, S., Jockusch., B.M. and Jockusch., H. (1999) A role for polyproline motifs in the spinal muscular atrophy protein SMN. *J. Biol. Chem.*, **274**, 37 908–37 9l4.
57. Lorson, C.L. and Androphy, E.J. (1998) The domain encoded by exon 2 of the survival motor neuron protein mediates nucleic acid binding. *Hum. Mol. Genet.*, **7**, 1269–1275.
58. Bertrandy, S., Burlet, P., Clermont, O., Huber, C., Fondrat, C., Thierry-Mieg, D., Munnich, A. and Lefebvre, S. (1999) The RNA-binding properties of SMN: deletion analysis of the zebrafish orthologue defines domains conserved in evolution. *Hum. Mol. Genet.*, **8**, 775–782.
59. Crino, P.B. and Eberwine, J. (1996) Molecular characterization of the dentritic growth cone: regulated mRNA transport and local protein synthesis. *Neuron*, **17**, 1173–1187.
60. Aronov, S., Aranda, G., Behar, L. and Ginzburg, I. (2001) Axonal Tau mRNA localization coincides with Tau protein in living neuronal cells and depends on axonal targeting signal. *J. Neuroscience*, **21**, 6577–6587.
61. Zhang, H.L., Eom, T., Oleynikov, Y., Shenoy, S.M., Liebelt, D.A., Dictenberg, J.B., Singer, R.H. and Bassell, G.J. (2001) Neurotrophin-induced transport of a β-actin mRNP complex increases β-actin levels and stimulates growth gone mobility. *Neuron*, **31**, 261–275.
62. Kiebler, M.A. and DesGroseillers, L. (2000) Molecular insights into mRNA transport and local translation in the mammalian nervous system. *Neuron*, **25**, 19–28.
63. Mourelatos, Z., Abel, L., Yong, L., Kataoka, N. and Dreyfuss, G. (2001) SMN interacts with a novel family of hnRNP and spliceosomal proteins. *EMBO J.*, **20**, 5443–5452.
64. Rossoll, W., Kröning A.-K., Ohndorf, U.-M., Steegborn, C., Jablonka, S. and Sendtner, M. (2002) Specific interaction of Smn, the spinal muscular atrophy determining gene product, with hnRNP-R and gry-rbp/hnRNP-Q: a role for Smn in RNA processing in motor axons? *Hum. Mol. Genet.*, **11**, 93–105.
65. Patterson, P.H. (1992) Neuron-target interactions. In Hall, Z.W. (ed.), *An Introduction To Molecular Neurobiology.* Sinauer Sunderland, MA, pp. 430–431.
66. Greensmith, L. and Vrbova, G. (1996) Motoneurone survival: a functional approach. *Trends Neurosci.*, **19**, 450–455.
67. Lichtman, J.W., Burden, S.J., Culican, S.M. and Wong, R.O.L. (1999) Synapse formation and elimination. In Zigmond, M.J., Bloom, F.E., Landis, S.C., Roberts, J.L. and Squire, L.R. (ed.), *Fundamental Neuroscience*. Academic Press, New York, pp. 561–562.
68. Jablonka, S., Bandilla, M., Wiese, S., Buhler, D., Wirth, B., Sendtner, M. and Fischer, U. (2001) Co-regulation of survival of motor neuron (SMN) protein and its interactor SIP1 during development and in spinal muscular atrophy. *Hum. Mol. Genet.*, **10**, 497–505.
69. Ben Hamida, C., Soussi-Yanicostas, N., Butler-Browne, G.S., Bejaoui, K., Hentati, F. and Ben Hamida, M. (1994) Biochemical and immunocyto-chemical analysis in chronic proximal spinal muscular atrophy. *Muscle Nerve*, **17**, 400–410.
70. Lin, P., Kusano, K., Zhang, Q., Felder, C.C., Geiger, P.M. and Mahan, L.C. (1996) $GABA_A$ receptors modulate early spontaneous excitatory activity in differentiating P19 neurons. *J. Neurochem.*, **66**, 233–242.